1.16 μm InAs/GaAs Quantum Dot Laser grown by Metal Organic Chemical Vapor Deposition

Hao Liu, Qi Wang*, Zhiming Li, Jia Chen, Kai Liu and Xiaomin Ren
State Key Laboratory of Information Photonics and Optical Communications, Beijing University of Posts and Telecommunications, P.O.B. 66, 10, Xitucheng Road, Haidian District, Beijing 100876, People's Republic of China

(Received May 8, 2017; in final form May 10, 2018)

In this study, a 1.16 μm InAs/GaAs quantum dot laser operating at continuous wave condition grown by metal organic chemical vapor deposition was demonstrated. For the quantum dot laser diode with 2 mm cavity length and 10 μm stripe width bonded on a heat sink, continuous wave lasing can still be observed up to 55 °C. At room temperature, threshold current density was as low as 950 A/cm^2 and the output power reached 25.4 mW under 300 mA injection current ($1.58I_{th}$). In addition, the external differential efficiency of 43.1%, the internal quantum efficiency of 59.6% and the internal loss of 2.2 cm^{-1} have been obtained, respectively.

DOI: 10.12693/APhysPolA.134.508
PACS/topics: 42.55.Px, 81.15.Gh

1. Introduction

Self-assembled InAs quantum dots (QDs) have been attracting many researchers since the last century for their unique optical properties induced by the multiple dimensional size confinement [1–3]. Self-assembled InAs QDs have been used as active media in several kinds of active devices, such as lasers, superluminescent diodes and so forth [2–5]. Owing to the superior performance of QDs, semiconductor QD lasers can have extremely low threshold current density and temperature sensitivity [6, 7]. Generally speaking, there are two ways to grow semiconductor QD laser structures, i.e., molecular beam epitaxy (MBE) and metal organic chemical vapor deposition (MOCVD). Although many QD lasers grown by MBE or MOCVD have been demonstrated [6–12], it is still a challenge to grow QDs by MOCVD with a luminescence wavelength near or beyond 1.3 μm due to the formation of incoherent islands in the epitaxial process. However, as MOCVD growth is much more suitable for industrial application than MBE, researchers have been focusing on QDs with high optical quality grown by MOCVD and corresponding QD lasers which are operating under continuous wave (CW) mode at room temperature [12, 13].

Likewise, our group has been making effort to realize CW lasing operation of MOCVD-grown QD laser. In this work, we grow a laser structure containing five stacked layers of InAs/GaAs QD on vicinal GaAs substrate by MOCVD and realize the room-temperature operation at 1.16 μm. The peak wavelength of electroluminescence (EL) spectrum of laser diode is around 1.23 μm at a very low current ($\approx$ 2 mA), indicating that the QD laser operates at the excited state rather than the ground state.

*corresponding author; e-mail: wangqi@bupt.edu.cn

2. Experimental

2.1. Growth details

In this study, the QD laser structure was grown on a Si-doped n-GaAs (100) substrate with 2° miscut along [111] direction which was performed in a low pressure MOCVD vertical reactor at a total pressure of 100 Torr. Trimethylindium (TMIn), trimethylgallium (TMGa), trimethylaluminum (TMAl) and arsine (AsH_3) were used as group III and V precursors, respectively. Silane (SiH_4) and diethylzinc (DEZn) were adopted as n- and p-type dopants. Schematic illustration of the epitaxial structure is shown in Fig. 1. First, a 300 nm

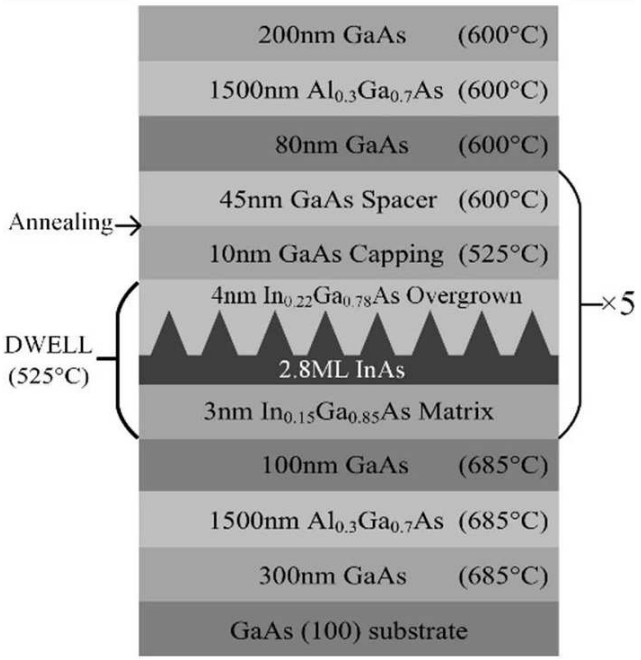

Fig. 1. Schematic illustration of QD laser structure.

thick n-GaAs buffer layer was deposited at the growth temperature (T_g) of 685 °C, followed by a 1.5 μm thick n-$Al_{0.3}Ga_{0.7}As$ cladding layer and a 100 nm thick undoped GaAs waveguide layer grown at the same T_g. The active region consisted of five layers of InAs QDs. Each QD layer was deposited at T_g of 525 °C on 3 nm thick $In_{0.15}Ga_{0.85}As$ matrix and overgrown with 4 nm thick $In_{0.22}Ga_{0.78}As$ strain-reducing layer (SRL), forming dot-in-a-well (DWELL) structures. InAs coverage is approximately 2.8 ML, the growth rate of InAs QDs is $\sim$ 0.03 ML/s and the employed V/III ratio is as low as 5. The density of QDs is around $3.5 \times 10^{10}/cm^2$. After InAs QDs were covered by additional 10 nm thick GaAs capping layer grown at 525 °C, a 15 s *in situ* annealing was performed under 525 °C with both TMGa and AsH_3 flow switched off by which the possible generated clusters were well dissolved, followed by 45 nm thick GaAs spacer layer deposited at the increased T_g of 600 °C to separate the adjacent QD layers. Then, T_g was ramped down to 525 °C again to grow the next QD layer. The remaining layer stacks including 80 nm thick undoped GaAs waveguide layer, 1.5 μm thick p-$Al_{0.3}Ga_{0.7}As$ cladding layer and a 200 nm thick p^+-GaAs contact layer were grown on the top of QD active region also at 600 °C to suppress the optical performance deterioration of QD active region.

2.2. Characterizations

As-grown QD laser structure was characterized by symmetric (004) double crystal X-ray diffraction (DCXRD), electrochemical capacitance voltage (ECV). The optical property of QDs was characterized by photoluminescence (PL). The characteristics of as-fabricated QD laser chips were measured by light-current-voltage (LIV) and electroluminescence (EL) system.

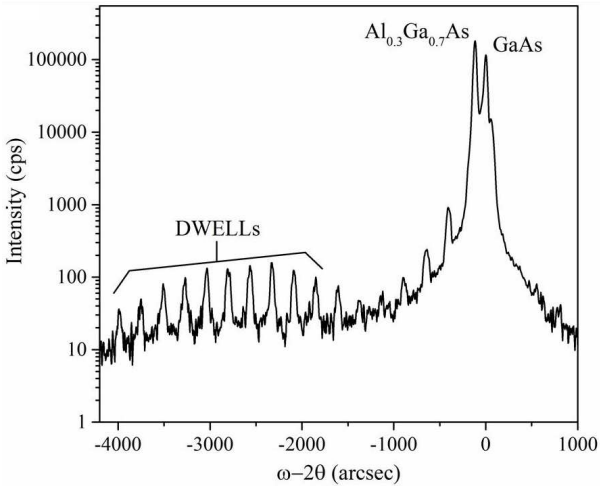

Fig. 2. (004) double crystal X-ray diffraction (DCXRD) rocking curve of QD laser structure.

Figure 2 shows the DCXRD (004) ω–2θ rocking curve of laser structure. GaAs buffer and waveguide as well as upper and lower $Al_{0.3}Ga_{0.7}As$ cladding layers can be easily distinguished from the curve. Owing to the thickness and position of $Al_{0.3}Ga_{0.7}As$ layers, the peak intensity of $Al_{0.3}Ga_{0.7}As$ is higher than that of GaAs. Meanwhile, in the curve, the satellite peaks on the left side of $Al_{0.3}Ga_{0.7}As$ peak which are clearly visible demonstrate the superior structural properties of as-grown multi-stacked DWELL layers.

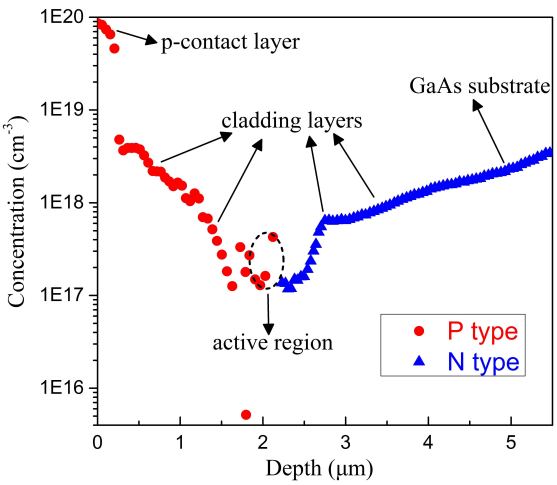

Fig. 3. Doping profile of the QD laser structure.

The doping profile of the laser structure measured by ECV is shown in Fig. 3. Si and Zn are used as the n-dopant and p-dopant in the growth process. As is shown in the profile, the doping concentration of GaAs contact layer ramped from about $10^{20}/cm^3$ to $4 \times 10^{19}/cm^3$ which is extremely high enough for the ohm contact. It is worth mentioning that when growing AlGaAs cladding layers at a relatively low temperature such as 600 °C, the carbon from TMAl may be a dopant which will incorporate into AlGaAs layer, resulting of a high doping concentration. Therefore, it is actually difficult to control the doping concentration of p-doping AlGaAs cladding layer under 600 °C. Here we used a ramped doping method to control the concentration and reduce the diffusion of zinc in p-doping AlGaAs cladding layer. From the doping profile we could see that the doping concentration of p-doped AlGaAs layer ranged from $4 \times 10^{18}/cm^3$ to $10^{17}/cm^3$.

2.3. Fabrication process

Following the standard photolithography process, the p-GaAs contact layer and p-$Al_{0.3}Ga_{0.7}As$ cladding layer were etched off by wet chemical etching (H_3PO_4:H_2O_2:H_2O) to fabricate ridge waveguide lasers. The ridges were then isolated with SiO_2 by plasma enhanced chemical vapor deposition (PECVD). Ti-Pt-Au was sputtered on the sample for p-side ohmic contact, then the wafer was thinned to about 100 μm followed by polishing, and AuGeNi-Au was evaporated for n-side electrode. Subsequently, the wafer was annealed in a rapid thermal annealing furnace for alloying. Finally, wafer was cleaved to laser chips without facet coating and then mounted on copper heat-sink to reduce significant current heating.

3. Results and discussion

Figure 4 shows the photoluminescent spectrum of the QD wafer with the upper p-doped GaAs and AlGaAs being etched, in which solid line is the measured PL spectrum while the dashed lines are the fitted curves. As we can see, the peak wavelength of the PL spectrum is around 1.22 μm, while it can be fitted by two Gaussian curves which indicate the ground state and the excited state. The peak wavelengths of the two fitted curves are around 1.22 μm and 1.15 μm, respectively. It is worth mentioning that the simple QD structure without upper AlGaAs and GaAs layers emits at around 1.24 μm, which implies the slight wavelength blue-shift of QD during the post growth. The full width of half maximum (FWHM) is around 103 nm, which is caused by the broad size distribution at QDs.

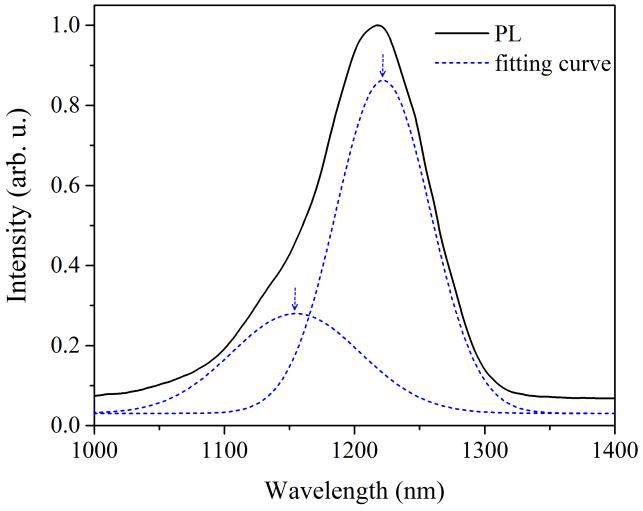

Fig. 4. PL spectrum of the QDs (solid line — measured PL curve, dashed line — fitting curve).

Figure 4 shows the LIV characteristics of the ridge laser with cavity length of 2 mm and ridge width of 10 μm, measured under CW conditions at room temperature. By fitting the I–V curve with a straight line shown in Fig. 5, we can obtain that the turn-on voltage is about 1.45 V, which is obviously higher than normal semiconductor lasers. The differential resistance is calculated by $\Delta V/\Delta I$ to be $\approx 2.6\ \Omega$, while the series resistance is $5.2\times10^{-4}\ \Omega\text{cm}^2$ which is relatively high. The reason may be that the doping profile of p-cladding layer ramped too fast which made the concentration relatively low. From the LIV curve, we can obtain that the threshold current is 190 mA, on account of the ridge width and cavity length, the corresponding threshold current density J_{th} equals to 950 A/cm^2. Moreover, we can obtain that the slope efficiency equals 231 mW/A (single facet), corresponding to external differential efficiency of 43.1% by using the following formula:

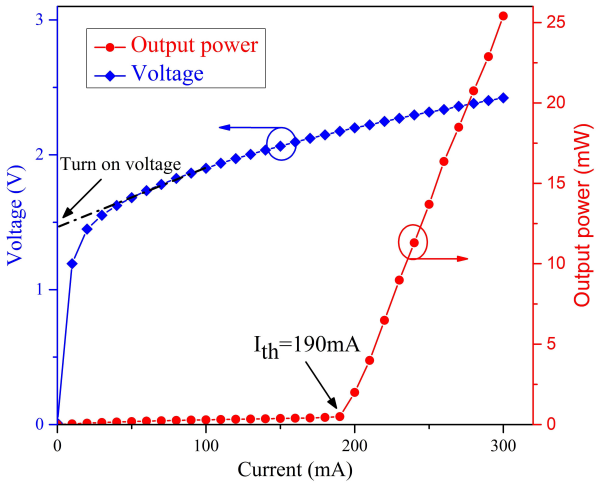

Fig. 5. LIV curve of the 2 mm cavity-length QD laser measured under CW mode at room temperature.

$$\eta_d = 2\frac{\Delta P}{\Delta l}\left(\frac{q\lambda}{hc}\right), \tag{1}$$

where $\Delta P/\Delta I$ is the slop efficiency of L–I curve, q is electronic charge, λ is photon wavelength, h is the Planck constant, and c is velocity of light. The output power of the laser chip is up to 25.4 mW at the current of 300 mA. When the cavity length of the laser chip is shortened to 1.5 mm, the threshold current density increased to 1133 A/cm^2, with a slope efficiency of 248.2 mW/A, corresponding to external differential efficiency of 46.3%. However, when the cavity length is shortened to 1 mm, the laser cannot operate in CW mode at room temperature, demonstrating that the maximum achievable optical gain of QDs is not high enough. By fitting the relationship between the external differential efficiency and the cavity length described by

$$\frac{1}{\eta_d} = \frac{1}{\eta_i}\left(1 - \frac{\alpha_i}{\ln R}L\right), \tag{2}$$

where R is the reflectivity of the cleaved facet which is assumed as 0.32, α_i is the internal loss, and L is the cavity length which could be 1.5 mm and 2 mm here. We could obtain that the internal quantum efficiency is 59.6% and the internal loss is 2.2 cm^{-1}.

We measured the light-current of the 2 mm cavity-length QD laser at different temperatures. Figure 6 reveals the temperature dependence. As the temperature increases, the threshold current density increases exponentially. The laser can still operate at CW mode until 328 K (55 °C), while the saturation power has degraded a lot. By fitting the relationship of temperature and threshold current density, the characteristic temperature of 49.1 K can be obtained.

Figure 7a shows the room temperature EL spectrum of QD laser at a very low current (2 mA). The peak wavelength of EL spectrum is around 1.23 μm. The FWHM of the fluorescence spectrum is $\sim$ 86 nm suggesting that the gain of the active region is broad, which is

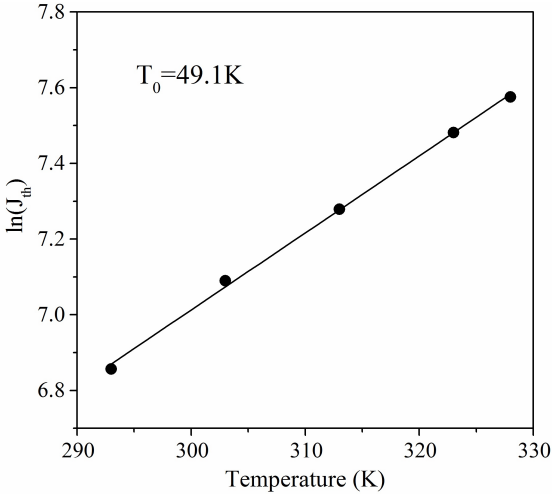

Fig. 6. $\ln(J_{th})$ vs. temperature of the 2 mm cavity-length QD laser.

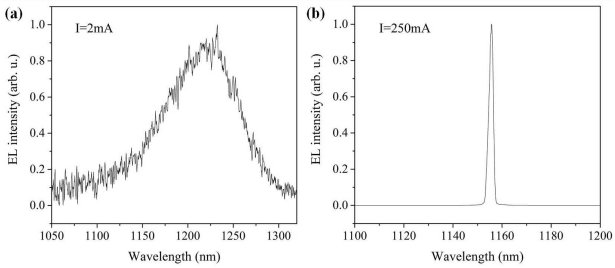

Fig. 7. EL spectra of the 2 mm cavity-length QD laser measured at different currents: (a) 2 mA, (b) 250 mA.

to say, the device needs more injected current to achieve the level of lasing. With the modal gain of the excited state higher than the ground state, when increases the injected current, the gain of ground state becomes saturated [14, 15], while the gain of the excited state enhances, resulting of an emitting wavelength of ~ 1.16 μm, which is corresponding to the excited state of QDs. The lasing spectrum at room temperature with injection current of 250 mA is shown in Fig. 7b, with emitting wavelength of 1155.7 nm and FWHM value of 2 nm.

4. Conclusion

In conclusion, we have demonstrated the MOCVD growth and characterizations of CW QD laser emitting at ~ 1.16 μm on vicinal GaAs (100) substrate. Under the cavity length of 2 mm and ridge width of 10 μm, the threshold current of the QD laser is 190 mA (the corresponding threshold current density of 950 A/cm^2), the external differential efficiency of 43.1% and the characteristic temperature of 49.1 K are also observed. Moreover, the internal quantum efficiency and the internal loss of the laser are calculated to be 59.6% and 2.2 cm^{-1}, respectively.

Acknowledgments

This work was supported by the National Natural Science Foundation of China (Nos. 61474008 and 61674020), Program for New Century Excellent Talents in University (NCET-13-0686), International Science & Technology Cooperation Program of China (No. 2011DFR11010) and the 111 Project (No. B07005). The authors would like to thank Haiqiao Ni of Institute of Semiconductors, Chinese Academy of Sciences for his valuable discussions.

References

[1] L. Chu, M. Arzberger, G. Böhm, G. Abstreiter, *J. Appl. Phys.* **85**, 2355 (1999).

[2] F. Heinrichsdorff, M. Mao, N. Kirstaedter, A. Krost, D. Bimberg, A. Kosogov, P. Werner, *Appl. Phys. Lett.* **71**, 22 (1997).

[3] S.S. Li, J.B. Xia, *J. Appl. Phys.* **88**, 7171 (2000).

[4] P. Lever, M. Buda, H.H. Tan, C. Jagadish, *IEEE J. Quantum Electron.* **40**, 1410 (2004).

[5] M. Rossetti, A. Markus, A. Fiore, L. Occhi, *IEEE Photon. Technol. Lett.* **17**, 540 (2005).

[6] H.Y. Liu, D.T. Childs, T.J. Badcock, K.M. Groom, *IEEE Photon. Technol. Lett.* **17**, 1139 (2005).

[7] O.B. Shchekin, D.G. Deppe, *Appl. Phys. Lett.* **80**, 3277 (2002).

[8] A.R. Kovsh, N.A. Maleev, A.E. Zhukov, S.S. Mikhrin, A.P. Vasil'ev, E.A. Semenova, Y.M. Shernyakov, M.V. Maximov, D.A. Livshits, V.M. Ustinov, N.N. Ledentsov, D. Bimberg, Z.I. Alferov, *J. Cryst. Growth.* **251**, 729 (2003).

[9] L. Yue, G. Qian, C.F. Cao, J.Y. Yan, Y. Wang, R.H. Cheng, S.G. Li, *Chin. Opt. Lett.* **11**, 061401 (2013).

[10] A. Passaseo, M.D. Vittorio, M.T. Todaro, I. Tarantini, M.D. Giorgi, R. Cingolani, A. Taurino, M. Catalano, A. Fiore, A. Markus, J.X. Chen, C. Paranthoen, U. Oesterle, M. Ilegems, *Appl. Phys. Lett.* **82**, 3632 (2003).

[11] T.D. Germann, A. Strittmatter, Th. Kettler, K. Posilovic, U.W. Pohl, D. Bimberg, *J. Cryst. Growth.* **298**, 591 (2007).

[12] D. Guimard, M. Ishida, D. Bordel, L. Li, M. Nishioka, Y. Tanaka, M. Ekawa, H. Sudo, T. Yamamoto, H. Kondo, M. Sugawara, Y. Arakawa, *Nanotechnology* **21**, 105604 (2010).

[13] Z. Qi, S. Li, S. Sun, W. Zhang, W. Ye, *J. Electron. Mater.* **45**, 661 (2016).

[14] J. Tatebayashi, N. Hatori, M. Ishida, H. Ebe, M. Sugawara, Y. Arakawa, H. Sudo, A. Kuramata, *Appl. Phys. Lett.* **86**, 053107 (2005).

[15] L.V. Asryan, M. Grundmann, N.N. Ledentsov, O. Stier, R.A. Suris, D. Bimberg, *IEEE J. Quantum Electron.* **37**, 418 (2001).